Self-Assembled Vesicular Nanostructures of Perylene End-Capped Poly(dimethylsiloxane)

Dianjun Yao, Timothy P. Bender,† Paul J. Gerroir,† and Pudupadi R. Sundararajan*

Department of Chemistry, Carleton University, 1125 Colonel By Drive, Ottawa, Ontario K1S 5B6, Canada

Received May 25, 2005; Revised Manuscript Received June 10, 2005

ABSTRACT: Self-assembly of the perylene segment leads to vesicle formation of perylene end-capped poly(dimethylsiloxane) (PDMS) in nonaqueous media. The perylene self-assembles into crystalline aggregate, with a well-defined melting temperature and reversible melting and crystallization. The T_m of the perylene aggregates increases with an increase in the length of the PDMS chain. The absorption spectra depend on the solvent used. TEM images show that a trilayer vesicle structure is formed with hexane mixtures. Thus, the packing of perylene depends on the choice of the solvent system. This initial attempt to prepare such vesicles in nonaqueous media may be applicable to similar systems.

Introduction

There has been significant activity on the self-assembly of amphiphilic block copolymers in solution.[1,2] One of the blocks is usually water-soluble, and a variety of morphologies such as spheres, rods, vesicles, and lamellae have been observed, depending on the composition of the polymer and the polarity of water. In a number of cases, the amphiphilic block copolymer has to be highly asymmetric. Such architecture involves a long, hydrophobic core-forming block and a short, hydrophilic corona block. It has been shown that for the case of polystyrene-*b*-poly(acrylic acid), with a relatively long PAA block, micelles are seen initially. With a progressive decrease in the length of the PAA segment, successive transitions were seen from micelles to vesicular structures.[1−7] The latter have hollow spherical shape, with walls composed of bilayers of the polymers.

Formation of such micelles or vesicles in nonaqueous media has not been explored so far. In this paper, we discuss the synthesis, morphology, and spectral properties of perylene end-capped poly(dimethylsiloxane) (PDMS). This is essentially an oligomeric PDMS linked at one end to a perylene unit, whereby the macromolecular structure resembles that of a surfactant. However, in this case the surfactant has a large planar π-system (whose stacking tendency and hence insolubility are well-known) attached to a long flexible, elastomeric and soluble PDMS chain. The micelle or inverse micelle formation in surfactant systems, depending on the nature of the headgroup, is well-known. It was expected that in nonaqueous media the self-assembly of the perylene units would lead to morphologies similar to those observed in the case of polystyrene-*b*-poly(acrylic acid) and similar block copolymer systems.

Among the various classes of pigments, perylene bisimides are remarkable in the diversity of colors that can be achieved in the solid by derivitization and the resulting changes in the π overlap and the crystal structure.[8] Perylene derivatives exhibiting liquid crystalline[9] or supramolecular polymer[10] characteristics have been studied. Perylenes have also been incorporated in polyimide polymers and copolymers.[11−14] Perylene derivatives are also used as photogenerators and n-type organic semiconductors for optoelectronic applications.[8] It is expected that vesicle formation of perylene derivatives could to lead to interesting and useful properties as such an assembly is analogous to the arrangement of perylene derivatives in a molecular crystal. This work is an initial attempt in this regard.

Experimental Section

3,4,9,10-Perylenetetracarboxylic acid dianhydride, 2,5-di-*tert*-butylaniline, zinc acetate dihydrate, imidazole, isoquinoline, and *tert*-butyl alcohol were purchased from Aldrich Chemical Co. and used as received. Amine-terminated poly(dimethylsiloxane)s (DMS-A11, DMS-A12, and DMS-A15) were purchased from Gelest Inc. and used as received. The molecular weights of PDMS terminated with primary amine end group were obtained by end-group titration, with aqueous HCl solution. The PDMS (0.1 mequiv) was stirred in 75 mL of 2-propanol, and an automated titrator was used. The molecular weight of each was determined as an average of three such measurements. The average molecular weights of A-11, A-12, and A-15 were determined to be 875, 1500, and 3035 amu, respectively. The synthesis of *N*-(2,5-di-*tert*-butylphenyl)-perylene-3,4-dicarboxylic imide (**1**) and perylene-3,4-dicarboxylic anhydride (**2**) (Figure 1) were carried out according to the literature procedure.[15]

Three different molecular weights of ~900, 1500, and 3000 of PDMS were used for the synthesis of **3**, **4**, and **5** (Scheme 1), respectively. In a round-bottom flask, 0.32 g (0.1 mmol) of perylene-3,4-dicarboxylic anhydride, 3.6 g (0.4 mmol) of amine-terminated poly(dimethylsiloxane) (DMS-A11), and 0.2 g of isoquinoline were dispersed in 15 mL of *m*-cresol, and the solution was slowly heated to 200 °C. The reaction mixture was stirred at 200 °C for 4 h, cooled to room temperature, and poured into 300 mL of methanol. The precipitated solid was filtered, repeatedly washed with aqueous sodium hydroxide (1 N) solution, followed by water and methanol, and dried to get the crude solid. It was dissolved in chloroform and then chromatographed with chloroform over silica gel. After evaporating the solvent and drying in a vacuum at 60 °C the yield was 1.05 g (86.1%) of M900. IR (KBr): 1692.5, 1649.8, 1594.8, 1379.7, 1354.9, 1250, 1094, 839.5, 809.1, 751.6.

M1500 (**4**) (with DMS-A12). IR (KBr): 1692.3, 1650.9, 1593.5,1379.8, 1355, 1259, 1094.9, 1060.4, 839.2, 809.2, 752.5.

M3000 (**5**) (with DMS-A15). IR (KBr): 1694.7, 1650, 1597, 1382, 1356.9, 1261.1, 798.5, 752.

† Xerox Research Centre of Canada, 2660 Speakman Drive, Mississauga, ON L5K 2L1, Canada.

* Corresponding author. E-mail: sundar@carleton.ca.

10.1021/ma051071r CCC: $30.25
Published on Web 07/09/2005

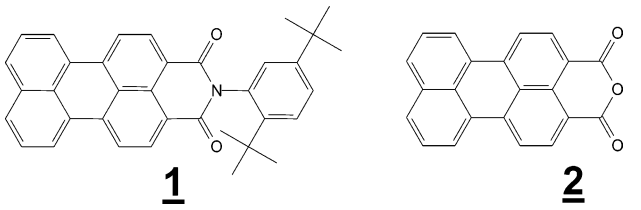

Figure 1. *N*-(2,5-Di-*tert*-butylphenyl)perylene-3,4-dicarboxylic imide (**1**) and perylene-3,4-dicarboxylic anhydride (**2**).

Scheme 1. Synthesis of Perylene End-Capped PDMS: (3) $n \approx 10$; (4) $n \approx 20$; (5) $n \approx 40$

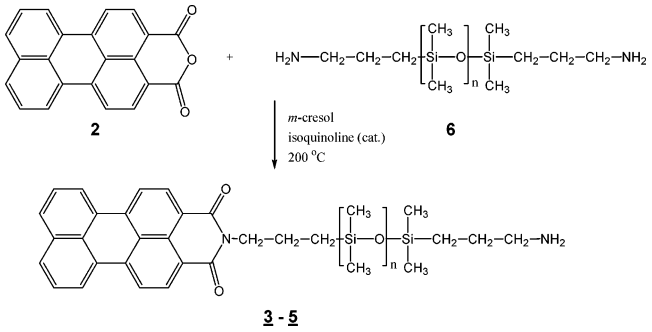

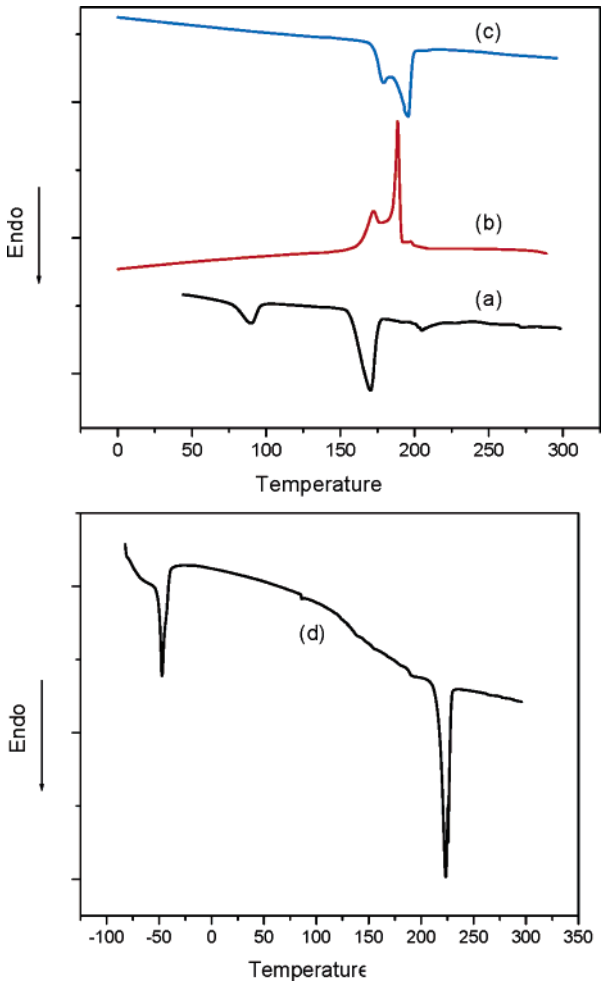

Figure 2. DSC thermograms of M900: (a) first heating, (b) cooling, and (c) second heating; (d) DSC thermogram (second scan) of M3000.

^{1}H NMR spectra were recorded on a Bruker-400 spectrometer using tetramethylsilane as an internal reference. Infrared measurements were performed on a Michelson M129 BOMEM FTIR spectrometer. A TA Instruments DSC Q100 was used for thermal analysis with a heating rate of 10 °C/min under nitrogen flow (50 mL/min). Thermal stabilities of the samples were determined using a Seiko 120 TG/DTA analyzer up to 500 °C at a heating rate of 10 °C/min under nitrogen flow (100 mL/min). UV−vis absorption spectra were recorded with a Perkin-Elmer 900 spectrophotometer. Fluorescence emission data were collected using a Shimadzu RF 1501 fluorescence spectrophotometer.

The X-ray diffraction patterns on film were recorded with a Statton-type Warhus flat film camera (William Warhus Co., Wilmington, DE), under vacuum, to eliminate air scatter, using Cu Kα radiation with a wavelength of 1.5418 Å. The diffractometer traces were obtained using a Philips PW1710 automated powder diffractometer (Cu Kα, λ = 1.5418 Å). The diffraction data were recorded from $2\theta = 2°$ to at least $2\theta = 40°$ with a step size of 1.2°/min. The data were analyzed using the Jade 5 XRD Pattern Processing software by MDI Materials Data Inc.

Transmission electron micrographs were recorded using a Philips CM20 TEM, operated at 120 kV. The samples were prepared by pipeting a small amount of the solution onto a carbon lacey grid. The solution was allowed to cascade down the surface of the tilted grid. This reduced the agglomeration of the material. The thin film formed in this manner was allowed to dry for a few hours before examination. This is similar to the protocol used for the TEM analysis of vesicular morphologies of block copolymers in aqueous media.[1−6] For cryo-TEM, the sample was placed on the grid as above, and the grid was then loaded into the cryo-holder and immediately inserted into the microscope. The reservoir of the cold stage initially at room temperature was filled with liquid nitrogen and kept filled throughout the duration of the sample examination. Once the temperature had dropped to −40 °C, the high tension was turned on and filament current increased to saturation. Micrographs were acquired between −40 and −55 °C.

Results and Discussion

Imides can be prepared in a single step by heating an anhydride and an amine together in a polar solvent such as NMP, DMAc, or *m*-cresol at high temperature. Imide−siloxane copolymers are prepared in a similar manner by copolymerization of a dianhydride, a diamine, and a siloxane-containing diamine.[16] In this paper we describe the synthesis and characterization of perylene end-capped poly(dimethylsiloxane) (PDMS) which has been made by reaction of perylene-3,4-dicarboxylic anhydride with an amino-terminated polysiloxane in *m*-cresol at elevated temperatures (compounds **3**−**5**, Scheme 1). We used a 4-fold excess of the amino-terminated polysiloxane so as to preferentially synthesize polysiloxanes that are end-capped at only one end with perylene moieties. The crude materials were washed by 1 N aqueous sodium hydroxide to change any unreacted perylene dicarboxylic anhydride to disodium perylene dicarboxylate and remove it. The column chromatography can remove trace amino-terminated PDMS and other unpurified materials. The reaction was monitored using FT-IR, by observing the wavenumber of carbonyl group shift from a broad peak between 1730 and 1780 cm^{-1} for the anhydride to peaks at 1690−1650 cm^{-1} upon imide formation. ^{1}H NMR ($CDCl_3$ solution) further confirmed the formation of perylene end-capped PDMS as chemical shifts between 8 and 8.6 ppm corresponding to perylene hydrogens and 0.7−4.2 ppm due to the hydrogens of the alkyl groups (α, β, and γ to the nitrogen atom), and chemical shifts lower than 0.5 due to hydrogens of the methyl groups attached directly to the silicon atoms were observed.

The question arises as to the possibility of both ends of the PDMS chain being substituted with perylene. As

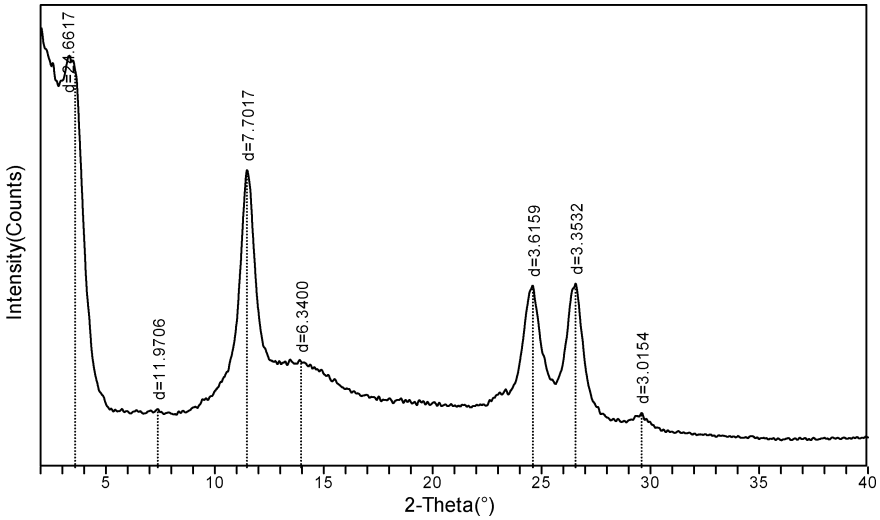

Figure 3. Powder X-ray diffractogram of M1500.

noted above, a 4-fold excess of amino-terminated polysiloxane was used. During the chromatographic separation process, the free amino-terminated main product would have higher interaction with the silica gel, and it will be the slower eluent compared to the product that reacted on both sides. ^{1}H NMR showed only the expected spectrum. The TLC plate also showed one eluent. The final product was easily soluble in most common solvents. This would not be the case if the perylene substitution occurred on the both ends of the polymer. Since amino-terminated PDMS is soluble in common solvents such as methanol and acetone, repeated wash with methanol would remove any unreacted amino-terminated PDMS. As an aside, repeated washing with 1 N aqueous sodium hydroxide is not expected to cause any scission of the Si—O bonds. This procedure has been used during the preparation of perylene-containing polymers with alkyl chains,[11,17] and it is known that the bond energy of the Si—O bond is ~5 kcal mol^{-1} higher that of the C—C bond.[18]

Crystallization and Melting Behavior. The as-prepared perylene end-capped PDMS was found to be semicrystalline. Figure 2 shows the DSC results on M900 and M3000. All three polymers (**3**−**5**) showed reversible melting and crystallization. M900 initially shows two melting transitions at 175 and 210 °C in the first scan (Figure 2a) and crystallization transitions upon cooling (Figure 2b). A similar occurrence of multiple melting peaks has been reported for other polymers.[19] It has been suggested[19b] that the low-temperature endotherm is due to the melting of crystals that exist prior to the heating scan and that the higher temperature endotherm is the result of melting of crystals formed by simultaneous melting and recrystallization (reorganization) during the DSC scan. The two melting endotherms become closer in the second scan (Figure 2c), with the peak position at 195 °C. M1500 and M3000 are also semicrystalline, with a T_m of 225 °C (as seen for the latter in Figure 2d). These results suggest the presence of molecular aggregation of the perylene units in the solid state and the resulting crystallinity. Note that the T_m of perylene by itself from its crystalline state is 278−280 °C.[20] The lower melting temperatures observed here is due to the less perfect ordering of the perylene units relative to its single crystal.

We observe that the T_m of the perylene in M900 is lower than in the case of M3000. It would seem that the longer, flexible PDMS segments facilitate aggregation of the perylene chain ends. This is corroborated by the heat of fusion as well. The value of ΔH, normalized for the weight fraction of perylene, is 80 J/g for M900, and it increases to 130 J/g for M1500 and M3000. It is known that perylene derivatives form liquid crystalline phases.[21] However, we do not observe consistent multiple transitions in this case on heating and cooling that would indicate such liquid crystalline transitions. In addition, Figure 2d shows a small melting endotherm at −50 °C, which is attributed to melting of the PDMS segment. This endotherm was not seen with the lower molecular weight samples (e.g., M900).

The X-ray diffraction trace from M1500 is shown in Figure 3. Four strong well-resolved reflections are seen, with d-spacings of 24.66, 7.70, 3.61, and 3.35 Å. The diffraction patterns from M900 and M3000 were similar. The 3.61 Å reflection corresponds to the π-stacking of the perylene and 7.70 Å to the side-to-side packing distance. The length of the perylene unit including the three CH_2 groups is about 12.3 Å, which is half the spacing at 24.66 Å. Thus, the three principal packing directions of the perylene unit are seen in the X-ray diffraction. Note that PDMS itself crystallizes only below −50 °C. The crystalline peaks seen in Figure 3 are due to perylene aggregation.

UV−vis Spectra. The UV−vis and fluorescence spectra were recorded in dichloromethane, chloroform, dichlorobenzene, carbon tetrachloride, and hexane as well as mixtures of hexane with the chlorinated solvents. The concentrations were 2.0×10^{-5}−2.0×10^{-6} M, depending on the molecular weight.

Figure 4 shows the UV−vis spectra from these solvents and their mixtures for M900 and M3000. There are two significant changes that occur with increasing ratio of hexane. First, the absorption peaks become sharper and the doublets become well resolved. This difference is pronounced when the spectra from dichloromethane are compared with those from hexane. Second, the absorption maxima blue shift by 7−9 nm. With M900 in dichloromethane, peaks occur at 503 and 481 nm, and the ratio of the intensities of these peaks is 1.092. With hexane, these peaks shift to 495 and 467 nm, respectively, with a ratio of 1.042. In addition, a

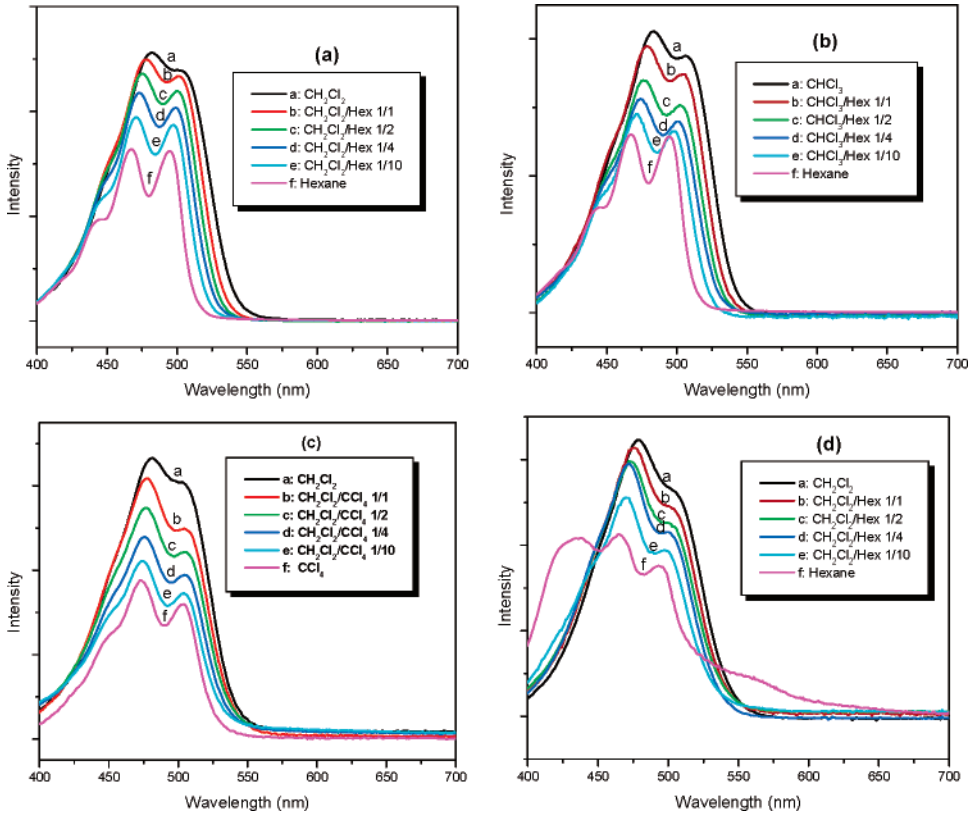

Figure 4. UV−vis spectra for M900 in (a) mixtures of dichloromethane and hexane, (b) mixtures of chloroform and hexane, (c) mixtures of dichloromethane and carbon tetrachloride; (d) M3000 in mixtures of dichloromethane and hexane.

third peak appears at 443 nm. The spectra for M1500 and M3000 in hexane also show the presence of the third peak at 443 and 438 nm, respectively. With chloroform, the peaks occur at 505 and 482 nm. These shift to lower wavelengths with increasing ratio of hexane. It was noted by Neuteboom et al.[14] that in the case alternating copolymers of perylene bisimide and poly(THF) in *o*-dichlorobenzene the blue shift of the absorption maximum is consistent with the formation of H aggregates.

Figure 4c shows the spectra from carbon tetrachloride, dichloromethane, and their mixtures. It is seen that although both are chlorinated solvents, the doublets in the spectra from CCl_4 are well-resolved compared to that in CH_2Cl_2. The nature of the solvent thus plays a role. The solubility parameter (δ) for PDMS is 14.9 $MPa^{1/2}$. Those for hexane, CCl_4, $CHCl_3$, and CH_2Cl_2 are 14.9, 17.6, 19, and 20.3 $MPa^{1/2}$, respectively, with increasing polarity.[22] Thus, the difference in δ between PDMS and hexane is close to zero, while it is large between PDMS and $CHCl_3$ or CH_2Cl_2. The interaction parameter χ between PDMS and hexane is 0.3−0.4, while it is 0.36, 0.6, and 0.69 with CCl_4, $CHCl_3$, and CH_2Cl_2, respectively.[22] The aggregation of the perylene segment would thus depend on the interaction between the solvent and PDMS. This is reflected in the vesicular morphology as seen from TEM.

Fluorescence spectra were recorded in the mixtures of dichloromethane and hexane. Figure 5 shows the fluorescent spectra for M900 and M1500. M3000 showed a similar spectrum. Excitation wavelength of 500 nm was used since all three compounds have strong absorption at that wavelength. Fluorescence spectra have a pattern very similar to UV absorption. With increasing the ratio of mixture of hexane and dichloromethane, the peaks shift to lower wavelength and the ratios of the lower and the higher wavelength peaks become larger.

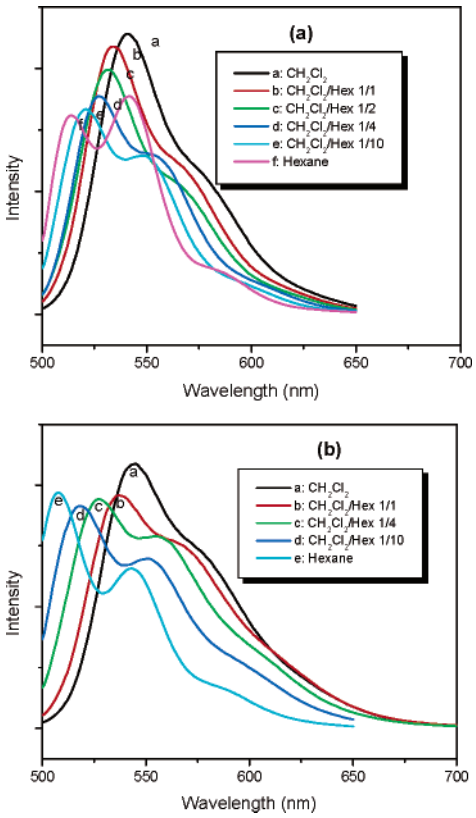

Figure 5. Comparison of fluorescent spectra in mixtures of dichloromethane and hexane for (a) M900 and (b) M1500.

Transmission Electron Microscopy. The intent in this article is to show that the perylene end-capped

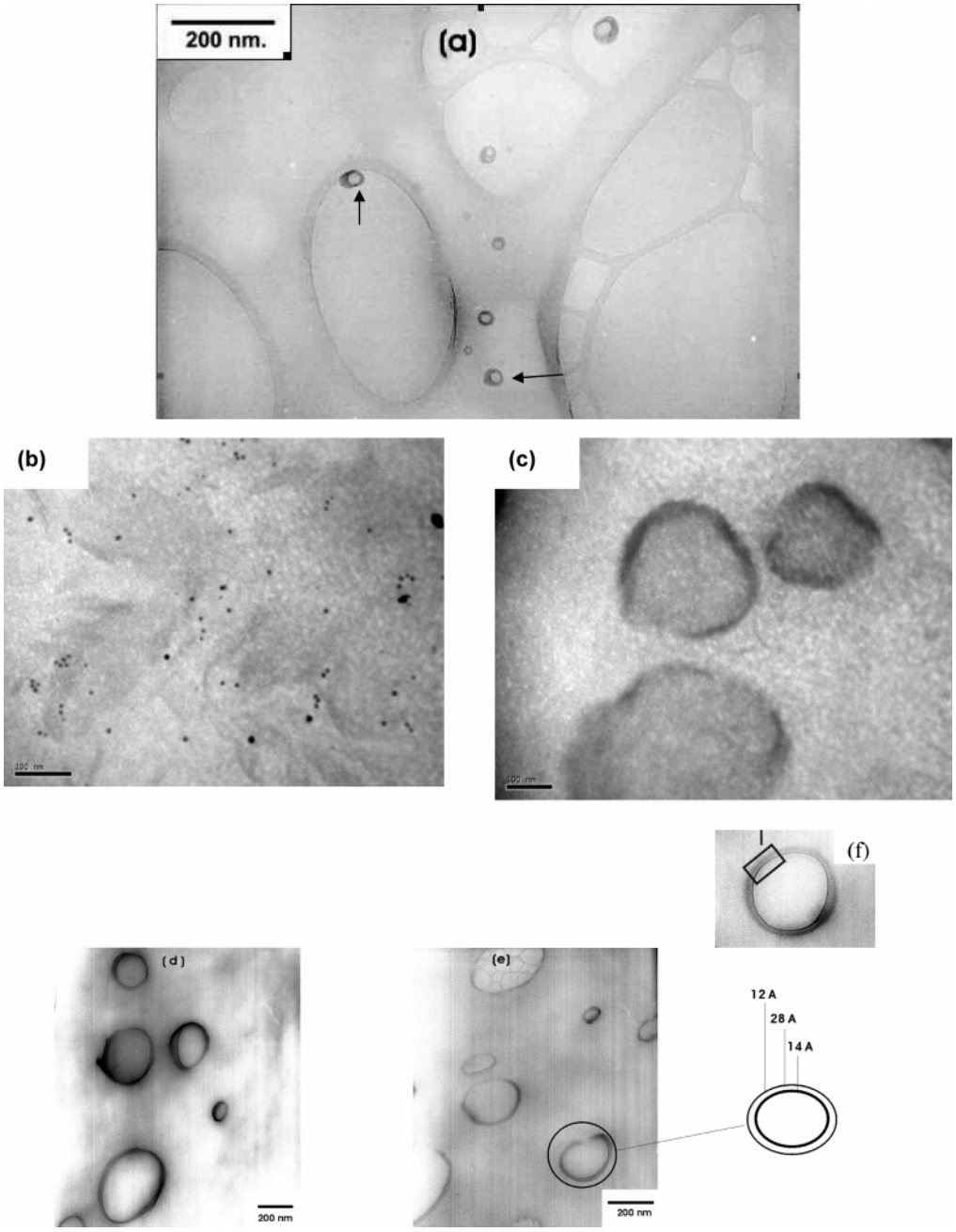

Figure 6. TEM images of (a) M900 in $CHCl_3$, (b, c) cryo-TEM image of M900 in $CHCl_3$, (d) M900 in CH_2Cl_2/hexane (50:50), and (e) M900 in hexane. (f) An enlarged view of a vesicle of M900 in hexane. The scale bars in (b) and (c) correspond to 100 nm.

PDMS forms micellar and vesicular morphology. It is realized that the method of sample preparation would have a significant influence on the observed morphology. The samples for TEM analysis were prepared in a manner similar to that used for studying the morphology of block copolymer vesicles in aqueous media.[1−6] The TEM micrographs are shown in Figure 6, including the cryo-TEM images of M900. For M900 from chloroform (Figure 6a), vesicles are seen (marked by arrows) with the dark region corresponding to PDMS surrounded by the shell formed by perylene. The interaction of the chlorinated solvent with perylene can be expected to be stronger than with PDMS. (The dark region is identified with PDMS due to the presence of the silicon atom. Note that the large "bubble-like" features are due to the lacey grid used for the TEM analysis and not to be confused with the vesicles.) These are similar to the morphologies observed in the case of equilibrium vesicular structures formed with PS_{300}-*b*-PAA_{44} in THF/water mixtures.[23] In that case, the size of the vesicles could be changed reversibly by changing the water content. In this initial study, only one concentration was used in each case. With M900 in chloroform, the size of the vesicle is about 30 nm, with a perylene layer thickness of about 2−3 nm. The structure of the vesicles from dichloromethane was similar.

With the cryo-image of M900 in chloroform (Figure 6c), the structure is similar to that shown in Figure 6a. The features are somewhat irregular, perhaps due to nonuniform solvent content. Although the same solvent was used, the size of the vesicles (100−300 nm) in Figure 6c is much larger than that of Figure 6a (∼30 nm). This demonstrates the diverse morphologies that the system could adopt, depending on the sample preparation and history. Such mixed morphologies, depending on solvation and other conditions, have been ob-

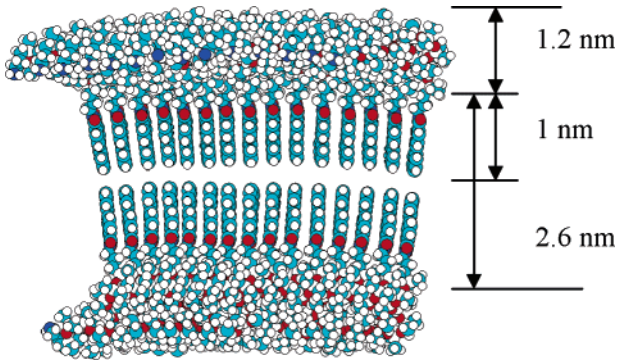

Figure 7. Trilayer packing model of perylene end-capped PDMS (from molecular mechanics modeling).

served in the cryo-TEM studies of surfactants[24,25] and PEO-based block copolymers.[26] These can also be compared with mixed morphologies obtained in the case of block copolymers.[1−6] With the same sample, some parts of the image appear micellar, as shown in Figure 6b. Note that PDMS crystallizes at the low temperatures used here (see DSC trace in Figure 2d). With M1500 and M3000 from chloroform, more aggregated compound vesicles were observed, perhaps due to association that develops in the solution. In the case of PS_{410}-*b*-PAA_{13}, these compound vesicle formation was attributed to nonequilibrium trapped morphologies.

The vesicles observed in the TEM image of M900 from the mixtures dichloromethane/hexane (Figure 6d) and chloroform/hexane (figure not shown here) and from hexane (Figure 6e) are larger than that from chloroform or dichloromethane. The vesicle diameters of M900 are about 240, 290, and 180 nm in chloroform/hexane, dichloromethane/hexane, and hexane, respectively. In fact, these seem to form a trilayer vesicle, with the perylene layer surrounded on either side by PDMS. A slightly enlarged view of a vesicle is shown in Figure 6f to show the dark/light/dark layers corresponding to PDMS/perylene/PDMS. This is different from the morphology observed with the chlorinated solvents. We attribute this to the favorable interactions between the PDMS and hexane. A schematic of the trilayer structure is shown as an inset in Figure 6. The PDMS layers are about 1.2 nm thick, and the perylene layer is 2.8 nm wide. A model based on a simple molecular mechanics simulation of this structure is shown in Figure 7. The length of the perylene segment is about 1.1 nm, and an edge-to-edge packing of the perylene would give rise to a spacing of about 2.6 nm. The perylene layer appears wider in some of images due perhaps to the sample preparation. As mentioned before, we followed the procedure similar to that of other authors for TEM analysis. Since a drop of the solution was cascaded on to the TEM grid, any dilation due to surface tension during drying could cause the layer to enlarge. Irrespective, the vesicle formation is clearly evident in the micrographs.

Figure 6 shows that the vesicles that formed with $CHCl_3$ or CH_2Cl_2 are much smaller compared to those formed with hexane or hexane mixtures, with (the dark region corresponding to) PDMS surrounded by the shell formed by perylene. It was discussed above that the difference in solubility parameters (and interaction parameters χ) is large between PDMS and $CHCl_3$ or CH_2Cl_2. This leads to the perylene forming the outer shell in this case. With hexane or hexane mixtures, the polarity decreases, and the difference in solubility parameters with PDMS is also very small. This causes the trilayer structure, with PDMS forming the outer and inner layers and the perylene segment sandwiched in between.

Conclusions

We have shown that the copolymer perylene end-capped PDMS, which is like a surfactant, forms vesicles in nonaqueous media. The perylene segment forms crystalline aggregate, with well-defined melting temperature and reversible melting and crystallization. The absorption spectra depend on the solvent used. Significant shifts in the absorption frequencies and changes in the relative intensities of the doublets are seen with the concentration of hexane in dichloromethane or chlorofrom. Thus, the packing of perylene can be changed by the choice of the solvent system. TEM images of the vesicles show a trilayer structure, depending on the solvent. These observations were rationalized on the basis of the solubility parameters of PDMS and those of the solvents as well as the interaction parameter χ between PDMS and the solvents used. This initial attempt to prepare vesicles in nonaqueous media has been successful and may be applicable to similar systems, e.g., with a noncrystallizable polymer such as poly(methylphenylsiloxane) and other types of photoactive/electroactive molecules. Part of the model for the trilayer structure shown in Figure 7 resembles the mushroom morphology described by Stupp et al.[27] for a rod−coil triblock molecule. Our study indicates that by varying the nature of the solvent different types of supramolecular nanostructures can be obtained, as envisioned by Stupp et al.[27]

Acknowledgment. Financial support from the Natural Sciences and Engineering Research Council Of Canada (NSERC) and Xerox Research Centre of Canada is gratefully acknowledged. D. Yao thanks the Government of Ontario, Canada for the Ontario Graduate Scholarship for Science and Technology (OGSST).

Supporting Information Available: ^{1}H NMR spectra of M900, M1500, and M3000. This material is available free of charge via the Internet at http://pubs.acs.org.

References and Notes

(1) Burke, S.; Shen, H.; Eisenberg, A. *Macromol. Symp.* **2001**, *175*, 273−283.
(2) Discher, D.; Eisenberg, A. *Science* **2002**, *297*, 967−973.
(3) Yu, K.; Eisenberg, A. *Macromolecules* **1996**, *29*, 6359−6361.
(4) Zhang, L.; Eisenberg, A. *Macromolecules* **1996**, *29*, 8805−8815.
(5) Zhang, L.; Eisenberg, A. *J. Am. Chem. Soc.* **1996**, *118*, 3168−3181.
(6) Yu, K.; Eisenberg, A. *Macromolecules* **1998**, *31*, 3509−3518.
(7) Massey, J.; Power, K. N.; Manners, I.; Winnik, M. A. *J. Am. Chem. Soc.* **1998**, *120*, 9533−9540.
(8) Law, K.-Y. *Chem. Rev.* **1993**, *93*, 449−486. Kazmaier, P. M.; Hoffmann, R. *J. Am. Chem. Soc.* **1994**, *116*, 9684−9691. Graser, F.; Hadicke, E. *Justus Liebigs Ann. Chem.* **1980**, 1994. Hadicke, E.; Graser, F. *Acta Crystallogr.* **1986**, *C42*, 189. Bender, T. P.; Duff, J. M.; Vong, C.; Hamer, G. K. US Patent 6,656,651B1, 2003. Hsiao, C.-K.; Hor, A.-M.; Duff, J. M.; Baranyi, G.; Allen, C. G. US Patent 6,051,351, 2000.
(9) Liu, S.-G.; Sui, G.; Cormier, R. A.; LeBlanc, R. M.; Gregg, B. A. *J. Phys. Chem. B* **2002**, *106*, 1307−1315.
(10) Arnaud, A.; Belleney, J.; Boué, F.; Bouteriller, L.; Carrot, G.; Wintgens, V. *Angew. Chem., Int. Ed.* **2004**, *43*, 1718−1721.
(11) Wang, Z. Y.; Qi, Y.; Gao, J. P.; Sacripante, G. G.; Sundararajan, P. R.; Duff, J. D. *Macromolecules* **1998**, *31*, 2075−2079.
(12) Ghassemi, H.; Zhu, J. H. *J. Polym. Sci., Polym. Phys.* **1995**, *33*, 1633−1639.

(13) Thelakkat, M.; Posch, P.; Schmidt, H.-W. *Macromolecules* **2001**, *34*, 7441−7447.
(14) Neuteboom, E. E.; Meskers, S. C. J.; Meijer, E. W.; Janssen, R. A. *Macromol. Chem. Phys.* **2004**, *205*, 217−222.
(15) Feiler, L.; Langhals, H.; Polborn, K. *Liebigs Ann.* **1995**, 1229−1244.
(16) Arnold, C. A.; Summers, J. D.; McGrath, J. E. *Polym. Eng. Sci.* **1989**, *29*, 1413−1418.
(17) Yao, D.; Wang, Z. Y.; Sundararajan, P. R. *Polymer* **2005**, *46*, 4390−4396.
(18) Pauling, L. *The Nature of the Chemical Bond*; Cornell University Press: Ithaca, NY, 1960; p 85.
(19) (a) Liu, S. L.; Chung, T. S.; Oikawa, H.; Yamaguchi, A. *J. Polym. Sci., Polym. Phys.* **2000**, *38*, 3018−3031. (b) Lee, Y.; Porter, R. S. *Macromolecules* **1987**, *20*, 1336−1341.
(20) O'Neil Maryadele, J.; Ed. *Merk Index*, 13th ed.; Merck & Co.: Whitehouse Station, NJ, 2001; p 7261.
(21) Cormier, R. A.; Gregg, B. A. *Chem. Mater.* **1998**, *10*, 1309. Struijk, C. W.; Sieval, A. B.; Dakhorst, J. E. J.; van Dijk, M.; Kimkes, P.; Koehorst, R. B. M.; Donker, H.; Schaafsma, T. J.; Picken, S. J.; van de Craats, A. M.; Warman, J. M.; Zuilhof, H.; Sudholter, E. J. R. *J. Am. Chem. Soc.* **2000**, *122*, 11057−11066.
(22) (a) Du, Y.; Xue, Y.; Frisch, H. L. In *Physical Properties of Polymers Handbook*; Mark, J. E., Ed.; American Institute of Physics Press: New York, 1996; Chapter 16. (b) Orwoll, R. A.; Arnold, P. A. Reference 22a, Chapter 14.
(23) Luo, L.; Eisenberg, A. *Langmuir* **2001**, *17*, 6804−6811.
(24) Hammarström, L.; Velikian, I.; Karlsson, G.; Edwards, K. *Langmuir* **1995**, *11*, 408−410.
(25) Zheng, Y.; Lin, Z.; Zakin, J. L.; Talmon, Y.; Davis, H. T.; Scriven, L. E. *J. Phys. Chem. B* **2000**, *104*, 5263−5271.
(26) Won, Y.-Y.; Brannan, A. K.; Davis, H. T.; Bates, F. S. *J. Phys. Chem. B* **2002**, *106*, 3354.
(27) Stupp, S. I.; LeBonheur, V.; Walker, K.; Li, L. S.; Huggins, K. E.; Keser, M.; Amstutz, A. *Science* **1997**, *276*, 384−389.

MA051071R